Dalton Transactions

PAPER

View Article Online
View Journal | View Issue

Cite this: *Dalton Trans.*, 2025, **54**, 2301

Donor-free 9-aluminafluorenes: molecular structures and reactivity†

Paula L. Lückert, Jannik Gilmer, Alexander Virovets, Hans-Wolfram Lerner and Matthias Wagner *

Received 11th November 2024,
Accepted 29th November 2024

DOI: 10.1039/d4dt03148b

rsc.li/dalton

Aluminum-doped polycyclic aromatic hydrocarbons (PAHs) are underexplored despite the broad applications of boron-containing PAHs in areas such as catalysis and optoelectronics. We disclose the donor-free, sterically unprotected 9-methyl-9-aluminafluorene (Me-AlFlu; **2**), synthesized by heating a 9,9-dimethyl-9-stannafluorene and $AlMe_3$ in hexanes. The compound is a dimer, $(\mathbf{2})_2$, with *trans*-positioned Al*Me* substituents in the solid state. In solution, $(\mathbf{2})_2$ shows a dynamic *cis*/*trans*-interconversion rather than a monomer-dimer equilibrium (Tol-d_8, RT). Lewis bases L cleave $(\mathbf{2})_2$ into monomeric adducts **2**·L (L = OEt_2, thf, pyridine). Lewis acidic $AlBr_3$ transforms $(\mathbf{2})_2$ into a 2,2′-$(Br_2Al)_2$-1,1′-biphenyl (**3**), crystallographically characterized as dimeric $(\mathbf{3})_2$. $(\mathbf{3})_2$ is a synthetic equivalent for the elusive free Br-AlFlu: Treatment with donor molecules furnishes Br-AlFlu·L adducts (L = OEt_2, pyridine); the three-coordinate, monomeric aluminafluorene Mes*-AlFlu was prepared from $(\mathbf{3})_2$, Mes*Li, and a 2,2′-dilithio-1,1′-biphenyl in quantitative yield (Mes* = 2,4,6-$(t\mathrm{Bu})_3C_6H_2$).

Introduction

Doping organic π-electron systems with other p-block elements is an effective strategy to impart new chemical and physical properties to these species.[1] Specifically, the combination of a polycyclic aromatic hydrocarbon (PAH) such as fluorene with boron as a dopant to generate 9-borafluorenes (BFlus) can have a particularly pronounced effect,[2,3] as a conjugation barrier (*i.e.*, the CH_2 fragment in the carbonaceous species) is removed and a vacant $B(p_z)$ orbital is introduced instead, which can now: (i) mediate electron delocalization and bring about novel optoelectronic properties,[4] (ii) facilitate reduction,[5,6] and (iii) act as a Lewis acid to promote bond-activation reactions[7] or the expansion of the five-membered central borole ring.[8]

Compared to the extensive research on BFlus, their heavier homologues, the 9-aluminafluorenes (AlFlus),[9,10] are far less well explored. This is unfortunate, because AlFlus are expected to exhibit a lower degree of aryl-heteroatom double-bond character than BFlus,[11] leading to a greater propensity to form structurally intriguing aggregates through Al⋯π(Ar) complexes or Al–C–Al′ two-electron–three-center (2e3c) bonds. Relative to open-chain arylaluminum compounds, AlFlus should possess a structurally enforced enhanced Lewis acidity due to their small endohedral C–Al–C angle. This angle (108° in a regular five-membered ring) deviates more from the ideal 120° angle of three-coordinate AlR_3 species than from the corresponding angles of perfectly tetrahedral (109.5°) adducts. By the same token, the behavior of Al-based Lewis acids is more diverse than that of their B-based counterparts, as Al sites, unlike B centers, can readily accommodate coordination numbers larger than four.

In 1962, Eisch *et al.* reported the formation of Ph-AlFlu through the metalative cyclization of *o*-biphenylyl(diphenyl)aluminum at 200 °C. Their claim was mainly based on the analysis of hydrolysis and iodinolysis products.[12,13] The topic lay dormant until 2015, when Chujo and Tanaka used salt-metathesis protocols to synthesize AlFlus carrying Al-bonded phenyl rings with one or two chelating (dimethylamino)methyl substituents at their *ortho* positions (Fig. 1). Their research focused on the emission properties of the obtained four- and five-coordinate AlFlus.[14,15] More recently, Braunschweig *et al.* disclosed the synthesis of various aluminafluorenes R-AlFlu [R = 1,2,4-$(t\mathrm{Bu})_3C_5H_2$ (92%; Fig. 1), $Ph_2(t\mathrm{Bu})Si$ (44%), 2-C_4H_3S (79%), *t*Bu (23%; Fig. 1), Br (53%)]. The compounds were again prepared from 2,2′-dilithio-1,1′-biphenyl by salt-metathesis reactions and isolated and structurally characterized as their ether adducts – with the exception of the η^5-cyclopentadienide derivative, which is monomeric in the solid state, and the *t*Bu derivative, which crystallizes as a dimer.[16]

Institut für Anorganische und Analytische Chemie, Goethe-Universität Frankfurt, Max-von-Laue-Straße 7, D-60438 Frankfurt, Main, Germany. E-mail: matthias.wagner@chemie.uni-frankfurt.de

† Electronic supplementary information (ESI) available: Synthetic procedures, NMR spectra, X-ray crystallographic data and computational details. CCDC 2394332–2394341. For ESI and crystallographic data in CIF or other electronic format see DOI: **https://doi.org/10.1039/d4dt03148b**

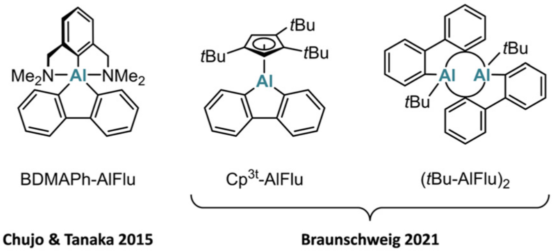

Fig. 1 Known mono- and dimeric 9-aluminafluorenes featuring 2,6-bis[(dimethylamino)methyl]phenyl (BDMAPh), 1,2,4-(tBu)$_3$C$_5$H$_2$ (Cp^{3t}), and *tert*-butyl (tBu) substituents.

One aim of our study outlined herein was to develop straightforward, high-yield synthesis protocols for base-free R-AlFlus featuring (i) the small substituent R = Me to minimize steric shielding of the Al center, and (ii) the reactive substituent R = Br for late-stage derivatization. Particular emphasis was placed on the molecular structure of Me-AlFlu in non-donor solvents and in the solid state, as well as on the synthesis of the first base-free, three-coordinate, monomeric aluminafluorene, Mes*-AlFlu (Mes* = 2,4,6-(tBu)$_3$C$_6$H$_2$). All our AlFlus were equipped with tBu groups in their 2,7-positions to enhance solubility in non-polar solvents and to facilitate NMR-spectroscopic analysis.

Results and discussion

Syntheses

The base-free Me-AlFlu (**2**) was synthesized by heating the 9,9-dimethyl-9-stannafluorene **1** with 1 equiv. of AlMe$_3$ [17] in either hexanes or C$_6$H$_6$/toluene (Scheme 1). The only by-product formed is the volatile and relatively inert SnMe$_4$.[18,19] An advantage of using hexanes as the solvent is that the dimer (**2**)$_2$ precipitates in pure form already upon cooling the reaction mixture to room temperature (yield: 74%); when C$_6$H$_6$/toluene is employed, the yield of (**2**)$_2$ is higher (91%), but some further workup is required. In the presence of the donor molecules Et$_2$O, THF, or pyridine, (**2**)$_2$ is cleanly split into its constituting monomers to furnish the monoadducts **2**·OEt$_2$, **2**·thf, or **2**·py (Scheme 1).

Treatment of (**2**)$_2$ with 4 equiv. of AlBr$_3$[17] in C$_6$H$_6$ results not only in quantitative AlMe/AlBr exchange but also in the incorporation of two AlBr$_3$ molecules to afford dimeric 2,2′-(Br$_2$Al)$_2$-1,1′-biphenyl [(**3**)$_2$, 95%; Scheme 1]. Upon addition of Et$_2$O to (**3**)$_2$ in C$_6$H$_6$, the donor adduct of Br-AlFlu, **4**·OEt$_2$, precipitates quantitatively as a colorless solid. In terms of yield, our overall synthesis cascade to **4**·OEt$_2$ improves upon the published protocol[16] by about 40 percentage points. Although pyridine can also reconstitute the AlFlu scaffold from (**3**)$_2$, it proved challenging to separate the target product **4**·py from by-products such as [AlBr$_2$(py)$_4$][X] ([**5**][X]; X = Br$^-$, AlBr$_4$$^-$; Fig. S44 and S45†).

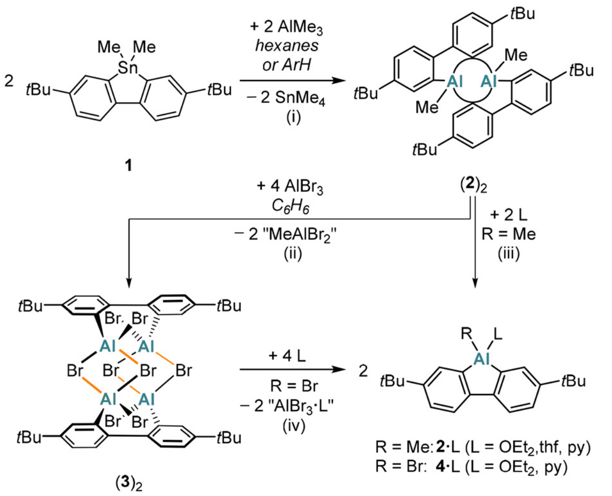

Scheme 1 Synthesis of donor-free (**2**)$_2$ through Sn/Al exchange between the 9-stannafluorene **1** and AlMe$_3$ (ArH: C$_6$H$_6$/toluene). The addition of AlBr$_3$ to (**2**)$_2$ furnishes (**3**)$_2$. Lewis bases (L: Et$_2$O, THF, or pyridine), cleave (**2**)$_2$ or (**3**)$_2$ into the monomeric adducts **2**·L or **4**·L. (i) Hexanes, 140 °C, 3 d (74% yield) or C$_6$H$_6$/toluene, 120 °C, 3 d (91% yield); sealed glass ampoule. (ii) C$_6$H$_6$, room temperature, 1 d (95% yield). (iii) **2**·OEt$_2$: in Et$_2$O, room temperature; **2**·thf: C$_6$D$_6$, room temperature; **2**·py: C$_6$H$_6$, room temperature (quantitative conversions). (iv) **4**·OEt$_2$: C$_6$H$_6$, room temperature (quantitative conversion); **4**·py: C$_6$D$_6$, room temperature (not isolated). Note: in (**3**)$_2$, four bonds were arbitrarily chosen as formally intermolecular (highlighted in orange) to facilitate the distinction between the monomers M and M′.

A particularly notable application of (**3**)$_2$ as a synthetic equivalent of donor-free Br-AlFlu is the preparation of Mes*-AlFlu (**6**): sequential addition of Mes*Li (4 equiv.) and 2,2′-dilithio-4,4′-di-*tert*-butyl-1,1′-biphenyl (2 equiv.) to (**3**)$_2$ in C$_6$H$_6$ gave **6** in 97% yield (Scheme 2).

Solid-state structures

In the solid state, Me-AlFlu forms centrosymmetric dimers, with the Al-bonded Me substituents adopting a *trans*-configuration (*trans*-(**2**)$_2$; Fig. 2).[20] The individual monomers, M and M′, are linked by two Al⋯C interactions, resulting in two Al(1)⋯Al(1)′ bridging aryl rings (Ar$_b$) and two terminal rings (Ar$_t$), with bridging [C(11)] and terminal [C(21)] *ipso*-C atoms. The position of Ar$_b$ is asymmetric between Al(1) and Al(1)′, as indicated by the differing angles Al(1)–C(11)⋯C(14) = 153.13(17)° and Al(1)′–C(11)⋯C(14) = 128.38(16)°. The fact that the

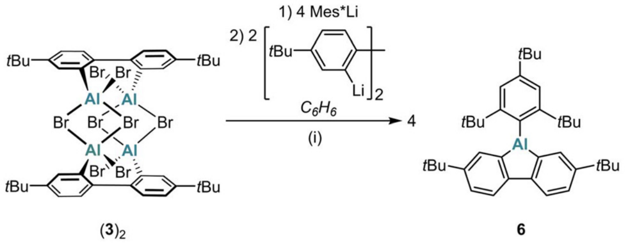

Scheme 2 Synthesis of Mes*-AlFlu (**6**) using (**3**)$_2$ as a synthetic equivalent of the elusive Br-AlFlu. (i) C$_6$H$_6$, room temperature, 1 d (97% yield).

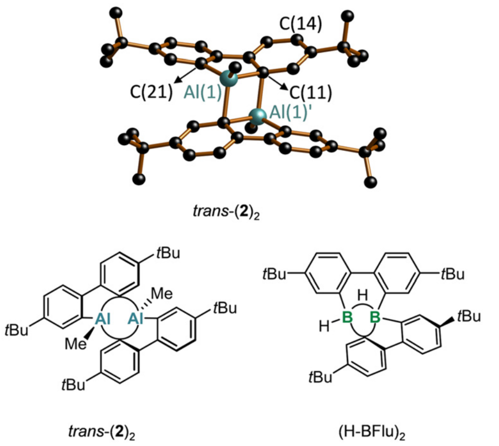

trans-$(\mathbf{2})_2$

trans-$(\mathbf{2})_2$ (H-BFlu)$_2$

Fig. 2 Top: molecular structure of *trans*-$(\mathbf{2})_2$ in the solid state; H atoms omitted for clarity (C: black, Al: turquoise). Bottom: structural formulae of *trans*-$(\mathbf{2})_2$ and of the comparable 9-borafluorene dimer (H-BFlu)$_2$.

Al(1)′–C(11)–C(14) angle is significantly closer to 90° than the Al(1)–C(11)–C(14) angle can still be viewed as a remnant of the initial intermolecular Al⋯π(Ar) complex when the two heterofluorene units first encountered each other. Correspondingly, the 'intermonomer' Al(1)′–C(11) bond (2.148(3) Å) is longer by 0.055 Å than the 'intramonomer' Al(1)–C(11) bond (2.093(3) Å; *cf*. Al(1)–C(21) = 1.971(3) Å). The range of C–C bond lengths in $\mathrm{Ar_b}$ (1.382(5)–1.427(5) Å) is close to that in $\mathrm{Ar_t}$ (1.389(5)–1.409(5) Å), indicating that the bridging mode does not lead to a systematic bond-length alternation. However, the two C–C bonds involving the bridging C(11) atom are slightly longer than the other four (1.409(4) and 1.427(5) Å *vs.* 1.382(5)–1.401(5) Å). Finally, we note that *trans*-$(\mathbf{2})_2$ has very similar structural parameters to Braunschweig's (*t*Bu-AlFlu)$_2$,[16] while the comparable 9-borafluorene dimer (H-BFlu)$_2$ shows one B–(μ-H)–B two-electron–three-center bond and one B⋯B′-bridging aryl ring (the three other rings remain terminally bonded).[21]

X-ray crystallography reveals that the compound $(\mathbf{3})_2$ no longer contains the 9-aluminafluorene motif but instead forms a centrosymmetric 2,2′-$(\mathrm{Br_2Al})_2$-1,1′-biphenyl dimer (Fig. 3). The two $\mathrm{Br_2Al}$ substituents in each monomer adopt an approximate *s-trans* configuration with a torsion angle Al(1)–C(11)–C(21)–Al(2) of 129.55(19)° [Al(1)–C(11) = 1.945(5) Å, Al(2)–C(21) = 1.956(4) Å]. Four Br atoms occupy bridging positions between Al centers of different monomers, assembling the cage-like structure of $(\mathbf{3})_2$. The underlying structural feature, a four-membered R(Br)Al–(μ-Br)$_2$–Al(Br)R ring, is common not only for aluminum tribromide (R = Br) but also for numerous dibromo(organo)alanes.[22]

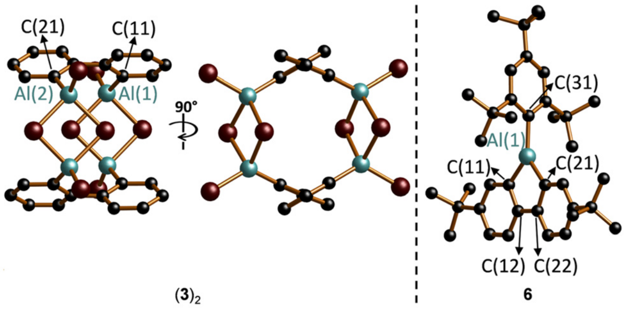

$(\mathbf{3})_2$ **6**

Fig. 3 Left: molecular structure of $(\mathbf{3})_2$ in the solid state, viewed from two different perspectives; *t*Bu-groups in the 2,7-positions of the biphenyl backbones and H atoms omitted for clarity. Right: molecular structure of **6** in the solid state; H atoms omitted for clarity (C: black, Al: turquoise, Br: brown).

The 2,4,6-$(t\mathrm{Bu})_3\mathrm{C_6H_2}$-substituted Mes*-AlFlu (**6**) exists as a monomeric species with a three-coordinate Al center in the crystal lattice (Fig. 3). The sum of C–Al–C angles is 360°, confirming a trigonal-planar ligand environment, although the endocyclic C(11)–Al(1)–C(21) bond angle is nearly rectangular (91.79(6)°). All three Al–C bonds are of equal length, regardless of whether they are endo- or exocyclic, or whether the respective *ipso*-C(p_z) orbital is positioned parallel or orthogonal to the vacant Al(p_z) orbital [Al(1)–C(11)/C(21)/C(31) = 1.9611(14)/1.9516(14)/1.9606(13) Å]. Within the five-membered $\mathrm{AlC_4}$ core, the length of the central C(12)–C(22) bond (1.5024(19) Å) approaches that of a typical C–C single bond (1.54 Å),[23] while the benzannulated bonds are significantly shorter [C(11)–C(12)/C(21)–C(22) = 1.4208(18)/1.4134(18) Å]. The other ten C–C bonds within the biphenyl fragment fall within a narrow range of 1.389(2)–1.4041(19) Å, closely matching the corresponding bonds in $\mathrm{C_6H_6}$ (1.39 Å).[24] Taken together, this analysis of bond lengths suggests that the AlFlu moiety of **6** preserves two largely unperturbed Clar sextets within its two $\mathrm{C_6H_3}$ fragments, with no indication of a delocalized (antiaromatic) π-system, nor any significant Al(1)═C(11)/C(21) double-bond character in the $\mathrm{AlC_4}$ heterocycle.

The donor adducts $\mathbf{2}\cdot\mathrm{OEt_2}$, **2**·py, and **4**·py were subjected to X-ray analysis to confirm that $(\mathbf{2})_2$ and $(\mathbf{3})_2$ can indeed serve as precursors of Me-AlFlu and Br-AlFlu, respectively (Fig. S40, S41, S43†). Furthermore, compared to donor-free **6**, the C–C bond lengths within the $\mathrm{C_6H_3}$–$\mathrm{C_6H_3}$ units of **2**·py and **4**·py were found to differ by no more than 3σ (and much less for most bonds).[25] This observation again suggests that the vacant Al(p_z) orbital exerts no significant electron-withdrawing mesomeric effect on the π-electron system.

NMR analysis

At room temperature, **2** gives severely broadened ^{1}H NMR signals, providing limited diagnostic value (Tol-d_8; Fig. 4 and S7†). At 70 °C, two sharp resonances are detectable in the aliphatic region of the spectrum (integral ratio 3H : 18H); the aromatic region contains one broad feature and two doublets with coupling constants of about 8.2 Hz (Fig. 4 and S6†). At −30 °C, the ^{1}H NMR spectrum of **2** is characterized by two well-resolved sets of signals attributable to two different but closely similar components (Fig. 4 and S8†); the same is true for the ^{13}C{^{1}H} NMR spectrum (Fig. S9†). The proton-integral values of the two sets indicate a minor-to-major component ratio of approximately 0.12 : 1 (Fig. S8†). Focusing on the major component, the ^{1}H NMR spectrum reveals one singlet at −0.67 ppm (6H), and two additional singlets at 1.47 and

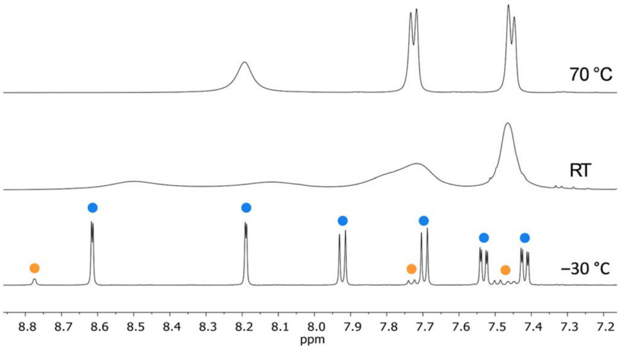

Fig. 4 Aromatic regions of ^{1}H NMR spectra of (**2**)$_2$ in Tol-d_8 (500.2 MHz). Top: 70 °C. Middle: room temperature. Bottom: −30 °C. 🔵: *trans*-(**2**)$_2$. 🟠: *cis*-(**2**)$_2$.

1.28 ppm (2 × 18H), assignable to two equivalent Al*Me* substituents and two pairs of non-equivalent *t*Bu groups, respectively. In the aromatic region, four doublets (4 × 2H; 2 × $^3J_{H,H}$ = 8.2 Hz, 2 × $^4J_{H,H}$ = 2.2 Hz) and two doublets of doublets (2 × 2H) are observed, indicative of two pairs of non-equivalent C_6H_3 fragments. In principle, these NMR features would align with both the molecular structure of the *cis*- and *trans*-(**2**)$_2$ dimer (as observed in the solid state). *Vice versa*, the minor signal set likely arises from *trans*- or *cis*-(**2**)$_2$. At low temperatures, both isomers are present in an (essentially) static mixture, while some dynamic rearrangement equilibrium is established at higher temperatures. This preliminary conclusion raises two questions: (i) Does *cis*- or *trans*-(**2**)$_2$ dominate at low temperatures? (ii) Is the dynamic equilibrium at high temperatures due to monomer/dimer association/dissociation, or is it the result of a rapidly interconverting *cis*/*trans* dimeric form of (**2**)$_2$?

To address question (i), quantum-chemical calculations predict that the crystallographically characterized *trans*-(**2**)$_2$ is 1.6 kcal mol^{-1} more favorable in energy than *cis*-(**2**)$_2$ (Scheme S1†; experimental value, determined at −30 °C from the proton-integral values of the minor/major component: $\Delta G°$ = 0.7 kcal mol^{-1}). Furthermore, the relative proportion of the minor component increases with solvent polarity, consistent with the existing dipole moment of *cis*-(**2**)$_2$ (^{1}H NMR spectroscopic control; Table S1 and Fig. S1, S2†). Finally, the computed ^{13}C chemical shift values for *cis*/*trans*-(**2**)$_2$ align more closely with the assumption that the major component is *trans*-(**2**)$_2$ rather than *vice versa* (Tables S9–S11†). It is therefore safe to assume that the major component in an equilibrating *cis*/*trans*-(**2**)$_2$ mixture is the *trans* isomer.

Regarding question (ii), we note that the computed energy required for cleaving *trans*-(**2**)$_2$ into its constituting monomers is 19.4 kcal mol^{-1} (in CH_2Cl_2). In contrast, the computed energy barrier of the *cis*/*trans* interconversion of (**2**)$_2$ is only $\Delta G^‡$ = 14.8 kcal mol^{-1}, which agrees well with the value of ≈14.5 kcal mol^{-1} experimentally determined from the coalescence temperature (T_c) in conjunction with the maximum peak separation ($\Delta\nu$) in the slow-exchange limit (CD_2Cl_2; see the ESI† for full details). The observed NMR features are therefore more convincingly attributed to a dynamic *cis*/*trans* equilibrium rather than to a monomer/dimer association/dissociation equilibrium.

In the temperature range of −30 to 70 °C, (**3**)$_2$ exhibited only extremely broadened signals in the ^{1}H and ^{13}C{^{1}H} NMR spectra, providing no structural information.

The ^{1}H and ^{13}C{^{1}H} NMR spectra of all adducts formed between our R-AlFlus and Lewis bases are in accord with the proposed molecular structures, as is the case for ligand-free **6** (see the ESI† for the fully assigned spectra). In addition to aiding in structure elucidation, ^{13}C{^{1}H} NMR spectroscopy is also a valuable tool for mapping the π-charge density distribution in conjugated systems, as the shielding of a specific C(sp^2) atom depends linearly on the corresponding π-electron density at that position.[26] Given this background, we compared the ^{13}C chemical shift values of the C atoms constituting the C_6H_3–C_6H_3 fragment of **6** with those of the equivalent atoms in the corresponding fragments of the adducts **2**·OEt$_2$, **2**·thf, **2**·py, **4**·OEt$_2$, and **4**·py. Except for the Al-bonded *ipso*-C atoms, whose shift differences varied from δ(**6**)–δ(adduct) = 3.3 to −4.7 ppm without a systematic trend, the $\Delta\delta(^{13}C)$ values for all other structurally analogous C atoms were less than ±1.8 ppm. In other words, we found no evidence of an overall ^{13}C-deshielding effect or π-electron depletion in **6** that could be attributed to a mesomerically electron-withdrawing Al(sp^2) center.

^{13}C{^{1}H} NMR spectroscopy on **2**·py and **4**·py provides a method to evaluate the relative Lewis acidities of free, monomeric Me-AlFlu and Br-AlFlu: in pyridine complexes of main-group elements, stronger acids induce increased shielding of the C-2,6 and deshielding of the C-3,4,5 nuclei of the ligand.[27] For **2**·py/**4**·py, our observations consistently indicate that Me-AlFlu is the stronger acid, comparable in this respect to BPh$_3$.[28] X-ray crystallography, however, offers a contrasting view: **4**·py exhibits a shorter Al–N bond and a more pyramidalized Al center, implying higher Lewis acidity for Br-AlFlu.[28] Given the small differences in the key NMR and structural parameters between **2**·py and **4**·py, these conflicting observations highlight the limitation of relying on a single method to determine Lewis acidity, emphasizing the need for complementary approaches.

Conclusions

We synthesized the donor-free 9-aluminafluorene Me-AlFlu (**2**), which was characterized as its dimer (**2**)$_2$ through X-ray crystallography and VT NMR spectroscopy (Tol-d_8). The key to this success was the highly selective reaction between the 9,9-dimethyl-9-stannafluorene **1** and AlMe$_3$,[17,18] which proceeds in non-donor solvents and releases volatile SnMe$_4$ as the sole by-product. Unlike the bulky *tert*-butyl group in *t*Bu-AlFlu,[16] the sterically less demanding methyl substituent in Me-AlFlu allows relatively unhindered access to the electrophilic Al center, as demonstrated by the straightforward formation of various base adducts **2**·L (L = OEt_2, thf, py). In terms of an umpolung of the Al center, exploring the reduction of **2** on a preparative scale could be promising (a non-benzannulated alumole has previously been reduced to its corresponding dianion).[10] The resulting product, $[\mathbf{2}]^{2-}$, could potentially serve as an Al-centered nucleophile – analogous to the $[\text{H-BFlu}]^{2-}$ dianion, which is a valuable B-centered nucleophile.[3,6,29]

Treatment of $(\mathbf{2})_2$ with $AlBr_3$ furnishes the 2,2′-$(Br_2Al)_2$-1,1′-biphenyl $(\mathbf{3})_2$. Although this ring-opened product no longer retains the AlFlu motif, it rearranges back to afford Br-AlFlu adducts, such as **4**·L (L = OEt_2, py), in the presence of Lewis bases. The use of Mes*Li, which provides the extremely bulky, negatively charged Lewis base $[\text{Mes*}]^-$, grants unprecedented access to three-coordinate, monomeric aluminafluorenes, specifically Mes*-AlFlu (**6**), *via* LiBr elimination. This reaction proves the utility of $(\mathbf{3})_2$ as a synthetic equivalent for the still-elusive free Br-AlFlu. A comparison of characteristic structural and NMR features of **6** with those of **2**·L/**4**·L reveals that the three-coordinate Al center exerts only a negligible π-electron withdrawing effect and does not mediate significant π-electron delocalization.

Author contributions

P. L. L. performed the experimental studies and characterized all new compounds. P. L. L. and J. G. performed the quantum-chemical calculations. A. V. performed the X-ray crystal structure analyses of all compounds. H.-W. L. and M. W. supervised the project. The manuscript was written by P. L. L. and M. W. and edited by all co-authors.

Data availability

The datasets supporting this article have been uploaded as part of the ESI.†

Conflicts of interest

There are no conflicts to declare.

Acknowledgements

The authors are grateful to Gabriele Sentis for performing all VT NMR measurements. We thank the center for scientific computing (CSC) Frankfurt and the University of Kent for providing HPC resources that contributed to the computational investigation of this work.

References

1 (*a*) A. Borissov, Y. K. Maurya, L. Moshniaha, W.-S. Wong, M. Żyła-Karwowska and M. Stępień, Recent Advances in Heterocyclic Nanographenes and Other Polycyclic Heteroaromatic Compounds, *Chem. Rev.*, 2022, **122**, 565–788; (*b*) M. Stępień, E. Gońka, M. Żyła and N. Sprutta, Heterocyclic Nanographenes and Other Polycyclic Heteroaromatic Compounds: Synthetic Routes, Properties, and Applications, *Chem. Rev.*, 2017, **117**, 3479–3716; (*c*) L. Ji, S. Griesbeck and T. B. Marder, Recent developments in and perspectives on three-coordinate boron materials: a bright future, *Chem. Sci.*, 2017, **8**, 846–863.

2 (*a*) X. Su, T. A. Bartholome, J. R. Tidwell, A. Pujol, S. Yruegas, J. J. Martinez and C. D. Martin, 9-Borafluorenes: Synthesis, Properties, and Reactivity, *Chem. Rev.*, 2021, **121**, 4147–4192; (*b*) E. von Grotthuss, A. John, T. Kaese and M. Wagner, Doping Polycyclic Aromatics with Boron for Superior Performance in Materials Science and Catalysis, *Asian J. Org. Chem.*, 2018, **7**, 37–53.

3 H. Budy, J. Gilmer, T. Trageser and M. Wagner, Anionic Organoboranes: Delicate Flowers Worth Caring for, *Eur. J. Inorg. Chem.*, 2020, 4148–4162.

4 (*a*) S. Yamaguchi, T. Shirasaka, S. Akiyama and K. Tamao, Dibenzoborole-Containing π-Electron Systems: Remarkable Fluorescence Change Based on the "On/Off" Control of the p_π–π* Conjugation, *J. Am. Chem. Soc.*, 2002, **124**, 8816–8817; (*b*) A. Wakamiya, K. Mishima, K. Ekawa and S. Yamaguchi, Kinetically stabilized dibenzoborole as an electron-accepting building unit, *Chem. Commun.*, 2008, 579–581; (*c*) A. Iida and S. Yamaguchi, Thiophene-Fused Ladder Boroles with High Antiaromaticity, *J. Am. Chem. Soc.*, 2011, **133**, 6952–6955; (*d*) A. Iida, A. Sekioka and S. Yamaguchi, Heteroarene-fused boroles: what governs the antiaromaticity and Lewis acidity of the borole skeleton?, *Chem. Sci.*, 2012, **3**, 1461–1466.

5 (*a*) A. Hübner, M. Bolte, H.-W. Lerner and M. Wagner, Extensive Structural Rearrangements upon Reduction of 9*H*-9-Borafluorene, *Angew. Chem., Int. Ed.*, 2014, **53**, 10408–10411; (*b*) A. Hübner, T. Kaese, M. Diefenbach, B. Endeward, M. Bolte, H.-W. Lerner, M. C. Holthausen and M. Wagner, A Preorganized Ditopic Borane as Highly Efficient One- or Two-Electron Trap, *J. Am. Chem. Soc.*, 2015, **137**, 3705–3714; (*c*) K. E. Wentz, A. Molino, S. L. Weisflog, A. Kaur, D. A. Dickie, D. J. D. Wilson and R. J. Gilliard, Stabilization of the Elusive 9-Carbene-9-Borafluorene Monoanion, *Angew. Chem., Int. Ed.*, 2021, **60**, 13065–13072; (*d*) H. Budy, T. Kaese, M. Bolte, H.-W. Lerner and M. Wagner, A Chemiluminescent Tetraaryl Diborane(4) Tetraanion, *Angew. Chem., Int. Ed.*, 2021, **60**, 19397–19405.

6 J. Gilmer, H. Budy, T. Kaese, M. Bolte, H.-W. Lerner and M. Wagner, The 9*H*-9-Borafluorene Dianion: A Surrogate for Elusive Diarylboryl Anion Nucleophiles, *Angew. Chem., Int. Ed.*, 2020, **59**, 5621–5625.

7 (*a*) P. A. Chase, W. E. Piers and B. O. Patrick, New Fluorinated 9-Borafluorene Lewis Acids, *J. Am. Chem. Soc.*, 2000, **122**, 12911–12912; (*b*) A. Hübner, A. M. Diehl, M. Bolte, H.-W. Lerner and M. Wagner, High-Temperature Reactivity of the Strongly Electrophilic Pristine

9*H*-9-Borafluorene, *Organometallics*, 2013, **32**, 6827–6833; (*c*) J. Gilmer, T. Trageser, L. Čaić, A. Virovets, M. Bolte, H.-W. Lerner, F. Fantuzzi and M. Wagner, Catalyst-free diboration and silaboration of alkenes and alkynes using bis(9-heterofluorenyl)s, *Chem. Sci.*, 2023, **14**, 4589–4596; (*d*) J. Gilmer, M. Bolte, A. Virovets, H.-W. Lerner, F. Fantuzzi and M. Wagner, A Hydride-Substituted Homoleptic Silylborate: How Similar is it to its Diborane(6)-Dianion Isostere?, *Chem. – Eur. J.*, 2023, **29**, e202203119.

8 (*a*) A. Hübner, Z.-W. Qu, U. Englert, M. Bolte, H.-W. Lerner, M. C. Holthausen and M. Wagner, Main-Chain Boron-Containing Oligophenylenes via Ring-Opening Polymerization of 9-H-9-Borafluorene, *J. Am. Chem. Soc.*, 2011, **133**, 4596–4609; (*b*) Y. Shoji, N. Tanaka, S. Muranaka, N. Shigeno, H. Sugiyama, K. Takenouchi, F. Hajjaj and T. Fukushima, Boron-mediated sequential alkyne insertion and C–C coupling reactions affording extended π-conjugated molecules, *Nat. Commun.*, 2016, **7**, 12704; (*c*) K. R. Bluer, L. E. Laperriere, A. Pujol, S. Yruegas, V. A. K. Adiraju and C. D. Martin, Coordination and Ring Expansion of 1,2-Dipolar Molecules with 9-Phenyl-9-borafluorene, *Organometallics*, 2018, **37**, 2917–2927; (*d*) Y. Murata, K. Matsunagi, J. Kashida, Y. Shoji, C. Özen, S. Maeda and T. Fukushima, Observation of Borane–Olefin Proximity Interaction Governing the Structure and Reactivity of Boron-Containing Macrocycles, *Angew. Chem., Int. Ed.*, 2021, **60**, 14630–14635; (*e*) T. Bischof, X. Guo, I. Krummenacher, L. Beßler, Z. Lin, M. Finze and H. Braunschweig, Alkene insertion reactivity of a *o*-carboranyl-substituted 9-borafluorene, *Chem. Sci.*, 2022, **13**, 7492–7497.

9 For selected publications on alumoles, the non-benzannulated congeners of AlFlus, see: (*a*) H. Hoberg and R. Krause-Göing, Darstellung und Eigenschaften von Pentaphenylaluminacyclopentadien, *J. Organomet. Chem.*, 1977, **127**, C29–C31; (*b*) T. Wasano, T. Agou, T. Sasamori and N. Tokitoh, Synthesis, structure and reactivity of a 1-bromoalumole, *Chem. Commun.*, 2014, **50**, 8148–8150; (*c*) T. Agou, T. Wasano, T. Sasamori and N. Tokitoh, Syntheses and Structures of Stable 1-Aminoalumole Derivatives, *Organometallics*, 2014, **33**, 6963–6966; (*d*) Y. Zhang, J. Wei, W.-X. Zhang and Z. Xi, Lithium Aluminate Complexes and Alumoles from 1,4-Dilithio-1,3-Butadienes and $AlEt_2Cl$, *Inorg. Chem.*, 2015, **54**, 10695–10700; (*e*) N. Tokitoh, T. Agou, T. Wasano and T. Sasamori, Synthesis and properties of stable alumoles, *Phosphorus, Sulfur, Silicon Relat. Elem.*, 2016, **191**, 584–587; (*f*) V. Y. Lee, H. Sugasawa, O. A. Gapurenko, R. M. Minyaev, V. I. Minkin, H. Gornitzka and A. Sekiguchi, 1-Chloroalumole, *Organometallics*, 2022, **41**, 467–471.

10 T. Agou, T. Wasano, P. Jin, S. Nagase and N. Tokitoh, Syntheses and Structures of an “Alumole” and Its Dianion, *Angew. Chem., Int. Ed.*, 2013, **52**, 10031–10034.

11 (*a*) T. D. Coyle, S. L. Stafford and F. G. A. Stone, Chemical and Spectroscopic Evidence for the Occurrence of π-Character in Carbon–Boron Bonds, *J. Chem. Soc.*, 1961, 3103–3108; (*b*) A. Foord, B. Beagley, W. Reade and I. A. Steer, A gas-phase electron-diffraction study of trivinylborane, *J. Mol. Struct.*, 1975, **24**, 131–137; (*c*) Y. Yamamoto and I. Moritani, Carbon-13 Nuclear Magnetic Resonance Studies of Organoboranes. The Relative Importance of Mesomeric B–C π-Bonding Forms in Alkenyl- and Alkynylboranes, *J. Org. Chem.*, 1975, **40**, 3434–3437.

12 J. J. Eisch and W. C. Kaska, The Novel Synthesis of Aluminoles by the Metalative Cyclization of Unsaturated Organoaluminum Compounds, *J. Am. Chem. Soc.*, 1962, **84**, 1501–1502.

13 J. J. Eisch and W. C. Kaska, The Synthesis of Aluminoles *via* the Addition and Cyclization Reactions of Arylaluminum Compounds, *J. Am. Chem. Soc.*, 1966, **88**, 2976–2983.

14 T. Matsumoto, H. Takamine, K. Tanaka and Y. Chujo, Synthesis and Characterization of Heterofluorenes with Five-coordinated Group 13 Elements, *Chem. Lett.*, 2015, **44**, 1658–1660.

15 T. Matsumoto, K. Tanaka, K. Tanaka and Y. Chujo, Synthesis and characterization of heterofluorenes containing four-coordinated group 13 elements: theoretical and experimental analyses and comparison of structures, optical properties and electronic states, *Dalton Trans.*, 2015, **44**, 8697–8707.

16 R. Drescher, L. Wüst, C. Mihm, I. Krummenacher, A. Hofmann, J. Goettel and H. Braunschweig, Synthesis, structure and insertion reactivity of Lewis acidic 9-aluminafluorenes, *Dalton Trans.*, 2021, **50**, 10400–10404.

17 We are aware that the compounds $AlMe_3$ and $AlBr_3$ are monomeric neither in solution nor in the solid state. However, for simplicity, the monomeric forms were used in calculating the quantities employed.

18 P. L. Lückert, J. Gilmer, A. Virovets, H.-W. Lerner and M. Wagner, Donor-free 9,10-dihydro-9,10-dialuminaanthracenes, *Chem. Sci.*, DOI: 10.1039/D4SC06940D.

19 $SnMe_4$ can in principle be recovered and used to recycle the Me_2SnCl_2 required to synthesize **1**.

20 Two polymorphs of $(Me\text{-}AlFlu)_2$ have been structurally characterized by X-ray diffraction: The denser α-form crystallizes in the triclinic space group $P\bar{1}$ with one unique molecule at a general position and a second molecule at an inversion center ($Z = 3$). The β-form, which is discussed in the main text, crystallizes in the monoclinic space group $P2_1/n$ with one crystallographically unique molecule at an inversion center. The key structural parameters of all the molecules are essentially identical (Fig. S39†); full details are available in the ESI.†

21 A. Hübner, M. Diefenbach, M. Bolte, H.-W. Lerner, M. C. Holthausen and M. Wagner, Confirmation of an Early Postulate: B–C–B Two-Electron–Three-Center Bonding in Organo(hydro)boranes, *Angew. Chem., Int. Ed.*, 2012, **51**, 12514–12518.

22 C. Elschenbroich, *Organometallics*, WILEY-VCH, Weinheim, Germany, 2006.

23 M. A. Fox and J. K. Whitesell, *Organic Chemistry*, Jones and Bartlett, Sudbury, Massachusetts, USA, 2003, p. 77.

24 E. D. Glendening, R. Faust, A. Streitwieser, K. P. C. Vollhardt and F. Weinhold, The Role of Delocalization in Benzene, *J. Am. Chem. Soc.*, 1993, **115**, 10952–10957.

25 The molecular structure of **2**·OEt_2 was excluded from this comparison due to its significantly larger error margins.

26 (*a*) M. Karplus and J. A. Pople, Theory of Carbon NMR Chemical Shifts in Conjugated Molecules, *J. Chem. Phys.*, 1963, **38**, 2803–2807; (*b*) R. H. Levin and J. D. Roberts, Nuclear magnetic resonance spectroscopy. Ring-current effects upon carbon-13 chemical shifts, *Tetrahedron Lett.*, 1973, **24**, 135–138; (*c*) H. Günther, H. Schmickler, H. Königshofen, K. Recker and E. Vogel, Does a “Ring Current Effect” Exist for ^{13}C-Nuclear Magnetic Resonance? A Study of Bridged Annulenes, *Angew. Chem., Int. Ed.*, 1973, **12**, 243–245; (*d*) D. G. Farnum, Charge Density-NMR Chemical Shift Correlations in Organic Ions, *Adv. Phys. Org. Chem.*, 1975, **11**, 123–175.

27 (*a*) A. Schnurr, M. Bolte, H.-W. Lerner and M. Wagner, Cyclic Phosphonium Bis(fluoroaryl)boranes – Trends in Lewis Acidities and Application in Diels–Alder Catalysis, *Eur. J. Inorg. Chem.*, 2012, 112–120; (*b*) M. Henkelmann, A. Omlor, M. Bolte, V. Schünemann, H.-W. Lerner, J. Noga, P. Hrobárik and M. Wagner, A free boratriptycene-type Lewis superacid, *Chem. Sci.*, 2022, **13**, 1608–1617.

28 $^{13}C\{^1H\}$ NMR data (the numbering scheme used here differs from that used in the ESI†): 147.3 (C-2,6), 125.0 (C-3,5), 139.9 (C-4) for **2**·py; 149.1 (C-2,6), 124.3 (C-3,5), 137.8 (C-4) for **4**·py; 148.3 (C-2,6), 125.6 (C-3,5), 141.0 (C-4) for BPh_3·py. X-ray analysis: Al–N = 1.9969(16)/2.0160(17) Å, N–Al–COG = 105.44/112.06° for two crystallographically independent molecules of **2**·py. Al–N = 1.964(2) Å, N–Al–COG = 122.26° for **4**·py. COG: centroid of the AlC_4 heterocycle.

29 H. Budy, S. E. Prey, C. D. Buch, M. Bolte, H.-W. Lerner and M. Wagner, Nucleophilic borylation of fluorobenzenes with reduced arylboranes, *Chem. Commun.*, 2022, **58**, 254–257.